How to Invent (or not Invent) the First Silicon MEMS Gyroscope

Marc S. Weinberg
Draper Laboratory
Cambridge, MA, USA[i]

***Abstract*—Draper designed and constructed traditional mechanical gyroscopes for Apollo and for strategic guidance systems. In 1984, Draper started the double gimbal gyro, which led to the silicon-on-glass tuning fork gyroscope that reported the first useful performance of a silicon MEMS gyroscope in 1992. This work became the basis for the successful Honeywell MEMS inertial measurement units and the starting point for other MEMS angular rate sensors.**

This paper will discuss considerations that were factored into the first tuning fork. These known factors included the thin, available proof masses, efficient mass use, quadrature stiffness, fluid gas "surf boarding", noise sources, frequency variation, and modal response. Unconsidered phenomena, such as glass charging, stiffness non-linearity, comb drive cross-coupling and electrical feed through, were designed around on the fly. Other fortuitous events such as material and parameter selection which avoided thermoelastic damping, which was not understood in MEMS until 2003, the limits of quadrature trimming, and the addition of key personnel, will be covered. In summary, demonstrating the first silicon MEMS gyroscope required well-applied engineering and a bit of serendipity.

Keywords— angular rate sensor; gyroscope; MEMS; tuning fork

I. Introduction

Draper's history and experience in developing the first practical silicon MEMS gyroscope is reviewed [1]. Major technical considerations are discussed. Major tuning fork gyroscope (TFG) technical considerations and physical principles are discussed.

All mechanical gyroscopes, including spinning wheels and vibrating rings, detect Coriolis acceleration, the product of angular velocity time linear velocity [2]. All have similar features and considerations. Examples include a motor to create the Coriolis velocity, placement of eigenmodes and frequencies, and large interference signals such as linear acceleration [3], quadrature terms, and electrical coupling.

TFG operation is shown in Fig. 1. When voltage is applied across the outer combs' gap, the proof masses are driven outward. The center combs' capacitance indicates the in-plane (drive) motion. Connecting the motor sense to the motor drive through appropriate electronics allows the proof mass to self-oscillate. The resulting velocity (defined relative to substrate) interacts with an in-plane angular rate (as shown), which causes (Coriolis) acceleration. With DC voltage applied to the sense electrodes (Section III.C), the output signal is current at the drive frequency in phase with drive velocity. Its amplitude is proportional to the input angular rate. Designing against signals in quadrature to the drive velocity are discussed in Section II.C.

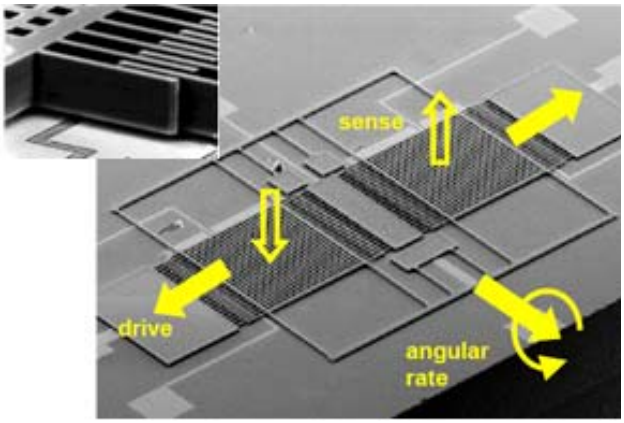

Fig. 1. TFG Operation and Details

This paper addresses the TFG's invention and development, which occurred in the early 1990s. Prior to the silicon MEMS TFG, Systron Donner developed the quartz angular rate sensor [4] which is still being refined and used for tactical applications. In 1984, Draper began working the double gimbal gyro [5]. After rudimentary demonstrations, this impractical gyro transitioned into the tuning fork gyro.

In 1992, the perceived applications were military tactical missiles and mortars and, perhaps, automobiles. Applications to mobile communication devices, computers, cameras, and games had not yet been foreseen.

In Section II, the knowledge base at the TFG beginning in 1992 is introduced. Section III introduces considerations that were engineered around. Facts that could have stalled the program, but were not known for many years, are introduced in Section IV.

II. 1991 TFG Knowledge

Based on experience with traditional mechanical and optical gyros and on the double gimbal gyro, TFG design was based on the following facts, assumptions, or rules of thumb.

[i] Draper Laboratory internally funded this work. "The views expressed are those of the author and do not reflect the official policy or position of the Department of Defense or the U.S. Government. Approved for Public Release, Distribution Unlimited."

978-1-4799-5915-0/15/$31.00 ©2015 IEEE

A. *Efficient Mass Use*

For large Coriolis force and scale factor, have as much mass as possible moving with maximum amplitude at the desired drive resonant frequency; that is, maximize the proof center of mass (CM) motion. Fig. 2 compares the proof mass center of mass available motion for the double gimbal versus tuning fork gyros. Worked with J. Bernstein, combining the comb drive with tuning forks was a break through. The TFG designed followed the rule of thumb that symmetry always helps. Examples include minimizing anchor losses and rejecting linear acceleration.

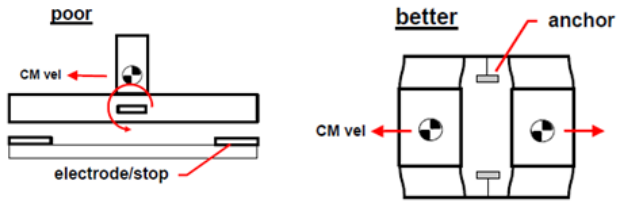

Fig. 2. Comparing Center of Mass Motion. Double gimbal (left) vs.TFG.

B. *Active Layer Thickness*

Our first plan was to follow UC Berkeley, whose polysilicon deposition for active layers was 1.5 to 2 µm. Draper desired 5 to 6 µm thickness because thicker generally leads to better performance. A second consideration: comb drives exert large lateral forces which nominally balance; however, mismatch causes sideways forces as depicted in Fig. 3 and, hence, bias errors. This error is reduced by extra suspension mass designs [6]. Setting sense and drive resonant frequencies (Section II.F) depended on different fabrication steps; nevertheless, Draper elected to drive in-plane and sense angular rate with vertical pick off as shown in Fig. 1.

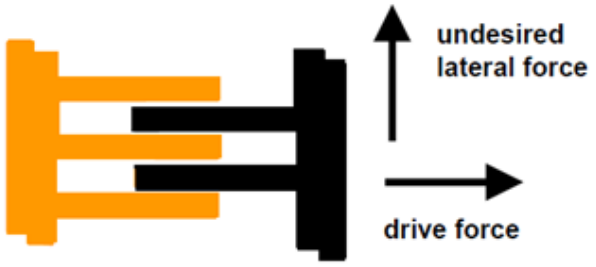

Fig. 3. Force Generated by Comb Drive

C. *Mechanical Quadrature*

Output signals in phase with drive displacement, not velocity, are quadrature signals which demodulation rejects; however, spill over, dynamic range, and limited authority of quad nulling loops required that as-built quadrature magnitude be restricted. For the TFG, rotated principal axes (Fig. 4) of the suspension beam cross section cause quadrature. The quadrature magnitude depends on design and aspect ratio. With the two proof mass TFG, RIE slant / parallelogram does not common mode.

Quadrature is controlled by careful micromachining, trimming, and quad nulling loop. Using a laser and partially automated stages, Draper trimmed initially. Examples are shown in Fig. 4. Removing (or adding) a corner modifies the area cross product of inertia and trims the parallelogram. With design changes and the advent of deep Reactive Ion Etching (RIE), Honeywell's commercial TFG products are not trimmed.

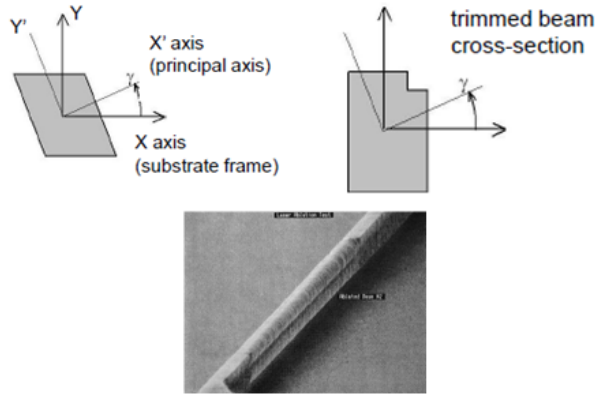

Fig. 4. Quadrature and Trimming in TFG. Upper left: typical beam cross section after RIE. Upper right: trim volume. Lower: beam after trimming.

D. *Hydrodynamic Coupling and Evacuation*

Tilted plates or proof masses and drive velocity cause hydrodynamic lift known as "surf-boarding." This lift, in-phase with drive velocity, is a rate bias dependent on gas viscosity and temperature. Relief holes (Fig. 1) and evacuation (Section III.F) reduce lift. Closed-form solutions for squeeze damping and lift with holes were developed. With relief holes and evacuation, hydrodynamic lift is a smaller effect than drive force coupling (Section III.B).

Besides reducing hydrodynamic coupling, evacuation is required in high performance gyros for the following reasons:

a. Reduce the electrostatic drive force, which pushes against damping, and, hence, coupling into sense axis force (Section III.B).

b. Maintain acceptable phase magnitude and stability between sense and drive axes. For low damping, the mechanical transfer function's change in phase with frequency is very steep.

c. Render Brownian motion small so that wide bandwidth resolution is achieved.

d. Enhance resolution. Low damping does not restrict sense axis motion.

E. *Noise sources*

Voltage noise in the pick-off preamplifiers and proof mass Brownian motion have dominated calculations of wide bandwidth noise through the present.

F. *Ordering Eigenfrequencies*

With two rigid masses, there are 12 modes. In advanced designs, proof mass compliance must be considered. Frequency placement is critical. Draper designs so that the following are lowest eigenfrequencies (Fig. 5):

a. *Drive or tuning-fork mode.* 10-25 kHz. Similar proof mass amplitudes are the design goal. The tuning fork design places both masses at the same (almost) anti-phase motion despite small differences in beam dimensions and reduces energy radiated to the substrate. To avoid acoustic interference, high audio frequency was selected.

b. *Translation mode*. Parallel motion should not be excited by electrostatic drive. Separating drive and translation frequencies by roughly 10% allows a good tuning fork mode with expected beam width tolerances.

c. *Sense mode*: To simplify electronics (no resonant frequency matching loops) and to realize scale factor magnitude and stability while modal frequencies vary, 5 to 10% sense-drive frequency variation became a rule of thumb.

d. *Out-of-plane mode*. The two proof masses move together perpendicular to the substrate.

With aging or temperature variation, the frequencies should not interfere with one another.

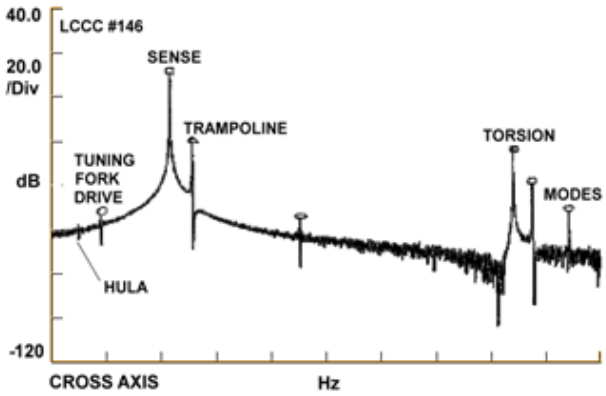

Fig. 5. Frequency response. Drive and pick off on sense axis.

III. Challenges Engineered on the Fly

As work progressed, new challenges emerged. With good work and propitious circumstances, solutions were found. Some of these topics contribute to the title's "how not to invent."

A. *The Silicon Glass Dissolved Wafer Process*

Our first plan was to extend the UC Berkeley polysilicon process to 6 μm thick moving parts. Before undertaking this development, TFG principles were demonstrated with electrodeposited nickel designs, which performed poorly because of metal's hysteretic stress-strain curve. A recent addition, Dr. Steven Cho, recognized that the parts could be built with the relatively simple and robust U. Michigan dissolved wafer process [7] with little development time or investment. The process used in the 1990s is shown in Fig. 6. The work was later modified to include upper sense plates for performance and robustness.

B. *Electrostatic Comb Forces*

Because of ground plane asymmetry, electrostatic drive force results in sense force. For stator combs at 1 V and moving combs and ground plane grounded, constant voltage lines are shown in Fig. 7. Although the two proof masses common mode reject, geometric tolerance asymmetry results in this lift-to-drive coupling being a dominant error since the drive force equals the thermally sensitive drive axis damping.

For very thin initial units, the lift force was sufficiently high that the gyro would lock onto the "trampoline" mode, rather than the desired tuning fork mode. Diagnosis was complicated by unexposed glass (not ground) below the combs in some units.

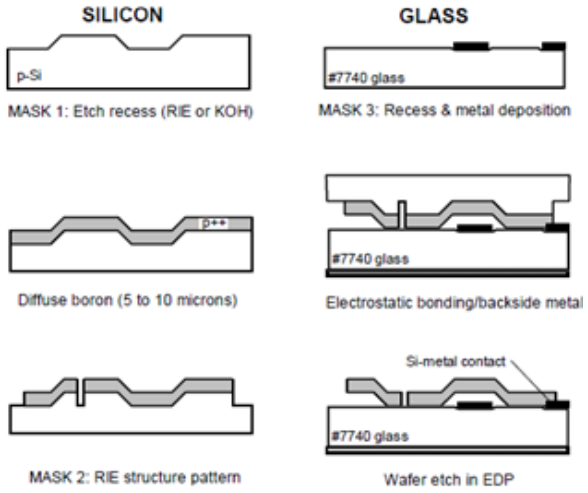

Fig. 6. Work Flow of the Dissolve Wafer Process

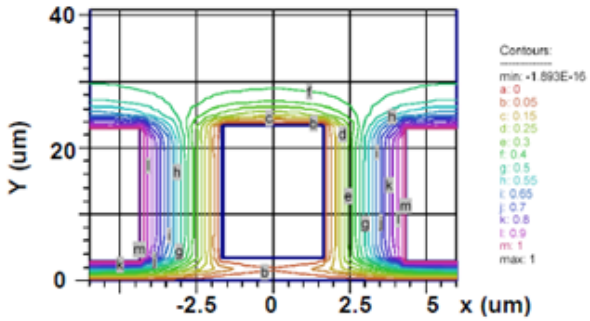

Fig. 7. Comb drive Constant Potential Contours

C. Glass Charging

When turned on, early units showed lengthy transients in scale factor. The moving proof mass could "see" exposed substrate glass not protected by electrodes of fixed potential AC ground. The sense plates and motor combs were excited with DC voltages while the proof mass virtually grounded. While the glass is highly resistive, the glass would eventually attain voltages determined by the nearby potentials.

Covering exposed glass near moving masses with deposited metal eliminated these charge transients. Although processing with overlapping metal was addressed, sense axis force rebalance was not pursued because of the inherent exposed glass.

D. Stiffness Nonlinearity

As the proof mass translates, the suspension beams' axial tension increases so that a cubic term emerges in the spring force vs. displacement, the now well known Duffing effect [8]. For straight beams, frequency changed with drive amplitude so that drive frequency crossed sense natural frequency and the drive motion collapsed. As seen in Fig. 1, strain relief was built into the flexures so that frequency crossing was avoided.

E. TFG Electrical Model

In addition to the capacitors defined by the combs, proof masses, and sense electrodes, Fig. 8 shows two of several possible stray or leakage capacitances (among much contributed by A. Kourepenis). The basic observation that all conductors are coupled to one another leads to the following design rules:

a. Square law electrostatic forcing allows motor drive at different frequency than sensing

b. The traces and excitations in the mechanism and electronics should be balanced to reduce unwanted coupling to motor sense and sense electrodes.

c. Because left and right proof mass drive displacements are not equal, the outer motor drive combs should be split into a plus and a minus group.

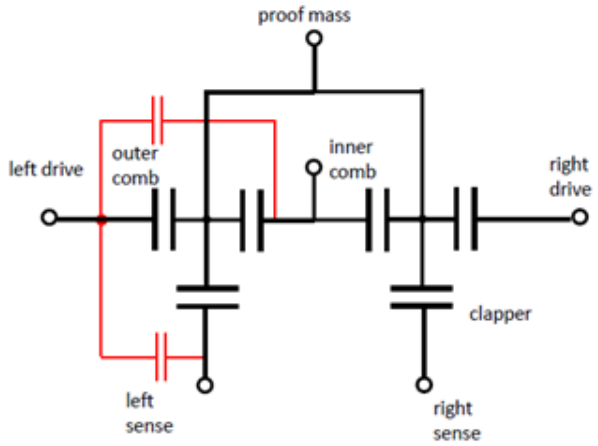

Fig. 8. TFG Mechanism Electric Schematic. Well defined capacitors are black and thick. Strays are red and thin.

F. Packaging

As a mechanism person, packaging is " the tail that wags the dog;" nevertheless, small packages able to hold a 1 mTorr vacuum for ten years were crucial and required significant investment for their development. Draper's Tom Marinis and Honeywell's Whit Slemmons quarterbacked the package development. Consistent with Section III.E, stray capacitances must be low or well-balanced. Draper's and Honeywell's commercial inertial sensor were packaged in leadless ceramic chip carriers with welded covers and deposited getters that were activated after evacuation and sealing.

G. Electronics

While the MEMS device is small, much capital was invested in developing high performance electronics architecture and the capability to design mixed signal Application Specific Integrated Circuits (ASICs), an effort led by Draper's Paul Ward. In addition to low stray capacitance and off-frequency drive (Section III.E), low noise, low phase shift, high impedance, low distortion amplifiers, high performance demodulators, and other circuitry were implemented [9].

IV. Good Fortune

Some phenomena, which could have stalled the program, were not known or considered in the early 1990s. The initial designs avoided these pitfalls.

A. Unknown Phenomena

Although analyzed in the 1930s, thermoelastic damping models were not applied to MEMS until 2003 [10]. The available material and machining geometry space naturally avoided thermoelastic damping. Low damping was required for low material forces and for low electrostatic drive forces needed for bias stability.

As discussed in Section II.C and Fig. 4, trimming worked well on parts less than 20 µm. The required material removal depended on the beam height squared and sidewall slope increased with beam height; thus, trimming 50 µm thick parts was much more difficult and yields were poorer.

B. Added Personnel

At several points, new people were added to the project as replacements (the dot com days) or because of new challenges or transition to commercial development. Some additions were more capable than predecessors or teammates while others were less capable. In most cases, experiences at other companies, groups, or schools pushed the project forward, often in step jumps.

V. Conclusions

Draper's history and experience in developing the first practical silicon MEMS gyroscope and major technical considerations were reviewed. Demonstrating a useful sensor required well-applied engineering and a bit of serendipity.

The basic design is still produced commercially and its principles have been applied to other successful MEMS gyros.

The first investment was demonstrating the gyro mechanism. Large investments in removing last errors, electronics, and vacuum packaging followed. Going from invention to commercial product was a large effort.

ACKNOWLEDGMENT

Many, too many to list here, at Draper, Rockwell, Boeing, and Honeywell contributed to the MEMS TFG development.

REFERENCES

[1] J. Bernstein, S. Cho, A. T. King, A. Kourepenis, P. Maciel, and M. Weinberg, "A Micromachined Comb-Drive Tuning Fork Rate Gyroscope," in *IEEE Micro Electro Mechanical Systems*, Fort Lauderdale, FL, 1993.

[2] A. Lawrence, *Modern Inertial Technology*. New York: Springer-Verlag, 1993.

[3] M. Weinberg and A. Kourepenis, "Error Sources in In-Plane Silicon Tuning Fork MEMS Gyroscopes," *JMEMS,* vol. 15, pp. 479-491, June 2006.

[4] A. M. Madni and R. D. Geddes, "A Micromachined Quartz Angular Rate Sensor for Automotive and Advanced Inertial Applications," *Sensors,* pp. 26-33, September 1999.

[5] B. Boxenhorn and P. Greiff, "A vibratory micromechanical gyroscope," in *Proc. AIAA Guidance Controls Conf*, 1988, p. 1033.

[6] J. A. Geen and D. W. Carow, "Micromachined Gyros," US Patent 6,505,511 B1, Jan. 14,, 2003.

[7] L. Spangler and K. Wise, "A New Silicon-on-Glass Process for Integrated Sensors," in *IEEE Sensor and Actuator Workshop*, Hilton Head, SC, 1988, pp. 140-2.

[8] A. H. Nayfeh and D. T. Mook, *Nonlinear Oscillations*. New York: John Wiley & Sons, 1979.

[9] P. Ward, "Electronics for Coriolis Force and Other Sensors," US Patent 5,481,914, January 9, 1996.

[10] A. Duwel, J. Gorman, M. Weinstein, J. Borenstein, and P. Ward, "Experimental Study of Thermoelastic Damping in MEMs Gyros," *Sensors and Actuators A,* vol. 103, pp. 70-75, 2003.